LAWRENCE
LIVERMORE
NATIONAL
LABORATORY

LLNL-CONF-403684

Long Duration Backlighter Experiments at Omega

A.B. Reighard, S.G. Glendinning, P.E. Young, W.W. Hsing, M. Foord, M. Schneider, K. Lu, T. Dittrich, R. Wallace, C. Sorce

May 8, 2008

High Temperature Plasma Diagnostics
Albuquerque, NM, United States
May 11, 2008 through May 15, 2008

Long Duration Backlighter Experiments at Omega[1]

A.B. Reighard,* S.G. Glendinning, P.E. Young, W.W. Hsing, M. Foord, M. Schneider, K. Lu, T. Dittrich, R. Wallace, and C. Sorce
Lawrence Livermore National Laboratory, Livermore, CA 94551
(Dated: July 7, 2008)

We have successfully demonstrated a 7.5 ns-duration pinhole-apertured backlighter at the Omega laser facility. Pinhole-apertured point-projection backlighting for 8 ns will be useful for imaging evolving features in experiments at the National Ignition Facility. The backlighter consisted of a 20 μm diameter pinhole in a 75 μm thick Ta substrate separated from a Zn emitter (9 keV) by a 400 μm thick high-density carbon piece. The carbon prevented the shock from the laser-driven surface from reaching the substrate before 8 ns and helped minimize x-ray ablation of the pinhole substrate. Grid wires in x-ray framing camera images of a gold grid have a source-limited resolution significantly smaller than the pinhole diameter due to the high aspect ratio of the pinhole, but do not become much smaller at late times. This work was performed under the auspices of the U.S. Department of Energy by Lawrence Livermore National Laboratory under Contract DE-AC52-07NA27344.

I. INTRODUCTION

Pinhole-apertured point-projection radiography [1] provides many advantages when backlighting targets used in high-energy-density physics experiments. Using a pinhole to aperture a point-projection backlighting source provides a bright source with constant resolution. This source is highly uniform because the spot profile does not depend on the detailed profile of the source, can provide high magnification images, and needs only a small emitter at the necessary intensity, so it can be fielded using less laser power or at higher intensity. This type of backlighter target has been used successfully in experiments with both gated and ungated imagers, usually with the laser source lasting from 0.1 to 1 ns [2–5].

A uniform, high-magnification backlighter in the energy range of 7-9 keV will be useful for imaging evolving features in experiments on the National Ignition Facility (NIF) [6]. NIF will be able to drive experiments for several nanoseconds, so demonstration of a backlighter that would be bright for up to 8 ns is important.

Pinhole-apertured point backlighters work by aperturing a small point source between the source and the target. The magnification of this image is set by the ratio of the image distance to the object distance. A diagram is shown in Figure 1. The resolution of the image is (1-1/M) times the aperture size for an infinitely thin pinhole substrate.

Several challenges must be overcome to extend the length of time that this type of backlighter can be used. While the source must be bright enough to achieve sufficient signal-to-noise with an appropriate resolution level for a given experiment, the x-ray source can also cause pinhole closure by heating the high-z pinhole substrate, which can then flow to block the aperture [7, 8]. X-ray induced pinhole closure had previously limited the useful experiment time of a 10 μm diameter pinhole to less than 3 ns. Lasers hitting the surface of the backlighter will cause a shock wave to propagate towards the high-z substrate, which can also cause hydrodynamic motion of the substrate and pinhole closure. This backlighter has a history of debris issues, and so a mitigation scheme must be in place to avoid damaging a detector on-axis with the tantalum surface normal direction [9].

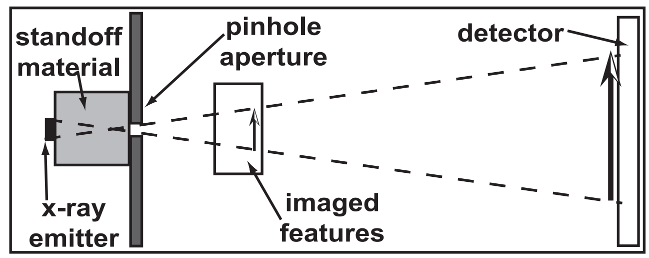

FIG. 1: Diagram of a pinhole-apertured point backlighter setup.

Here, we report successfully fielding an 8-ns duration backlighter on the Omega laser [10]. Framing camera images of the laser spot confirm that the source stays on and centered over the pinhole for 7.5 ns. Also at 7.5 ns, framing camera images of a resolution grid confirm adequate signal and minimal pinhole closure.

II. EXPERIMENT

The backlighter target consisted of 3 main components, like those shown on the left of Figure 1. The pinhole aperture was a 5 mm square, 75 μm thick tantalum substrate with a 20 μm pinhole which was coated with 5 μm parylene, which filled and tamped the pinhole. It is assumed that the thickness of the pinhole is completely filled with parylene. This substrate served as the x-ray aperture, and set the source-limited resolution element size. A 1

---

[1]Contributed paper, published as part of the Proceedings of the 17th Topical Conference on High-Temperature Plasma Diagnostics, Albuquerque, NM, May 2008.
*Electronic address: reighard2@llnl.gov

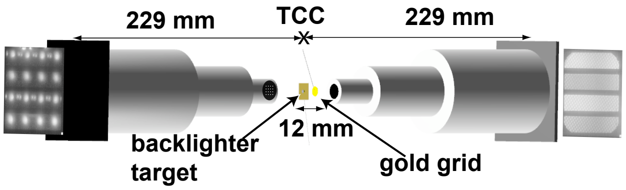

FIG. 2: Experimental setup. A framing camera aligned on axis with the target normal imaged the laser-driven spot on the zinc microdot, while another framing camera imaged the transmission of light through a gold resolution grid. The backlighter and grid targets are on separate target positioners. Typical data snapshots for each camera are shown near the image planes.

mm diameter, 400 μm thick high-density carbon (HDC) piece with a density of $\rho = 3.5$ g/cm^3 was attached to the tantalum substrate, centered over the pinhole. This component was designed to be thick enough to delay the shock from the laser drive from hitting the tantalum piece for at least 8 ns. A 150 μm square, 25 μm thick zinc foil was attached to the HDC piece, also centered over the pinhole in the tantalum substrate. This component was the source of x-rays, and emitted primarily He-α-like x-rays at 9 keV.

The use of a continuous substrate to separate the emitter from the pinhole helps mitigate the production of potentially dangerous shrapnel. Previous experiments used a vacuum gap between the emitter and pinhole [9]. In that setup, the laser-driven emitter was launched like a flyer plate at the pinhole substrate, colliding with it and generating large pieces of solid spall, which were launched directly at the detector. With a continuous substrate, debris is the result of a shock moving from the emitter, through the continuous stand-off substrate and into the tantalum, creating liquefied debris that is smaller in diameter and spreads out over a larger area. The HDC did attenuate the 9 keV He-α-like signal by 40%, resulting in a slightly lower x-ray flux through the pinhole.

A resolution grid was imaged by placing it between the pinhole substrate and a framing camera detector, 12 mm from the pinhole substrate. This gave an image magnification of 20. The grid was a 400-mesh gold grid, 3 mm in diameter. The wires were 33.5 μm wide and approximately 20 μm thick, with a 30 μm gap between the wires. The experiment configuration is shown in Fig. 2.

Twenty Omega beams were pointed at the zinc emitter material, with 10 kJ total laser energy. The beams had a 1 ns square pulse shape, and were individually delayed to give 2.6-2.9 x 10^{15} W/cm^2 of laser intensity for 7 ns, and 1.6 x 10^{15} W/cm^2 for an additional 1 ns. On these shots, there was no beam smoothing by phase plates or by spectral dispersion techniques. These beams hit the target in three cones of angles with respect to the target normal. Five of the twenty beams hit the target at an angle of 21°, another five beams hit the target at an angle of 42°, and the remaining ten beams hit the target at an angle of 58°. Groups of beams comprised primarily of 58° beams fire first, while beam groups with primarily 21° beams fire later in time. The 42° beams are interspersed throughout the pulses.

A four-strip framing camera [11, 12] on-axis with the target normal imaged the laser-driven zinc microdot. A 16-pinhole imager with 10 μm diameter pinholes was positioned to give 6x magnification onto the framing camera with a 200 ps pulse-forming module and 50 V reverse bias. The pinhole diameter sets the spatial resolution of the images, while the 200 ps pulsed voltage along the framing camera strip sets the time resolution and time separation of images on the same strip. This detector was filtered with 254 μm beryllium and 25.4 μm zinc, to exclude most of the signal from x-rays with energy below 5 keV.

On some shots, an additional two beams were pointed at gold patches attached to the sides of the HDC piece, at 200 kJ/beam in a 1 ns square pulse shape (see Figure 2 inset). These produced a bright, gold blow-off plasma which showed the position of the HDC edges on images of the laser driven spot, confirming the magnification of that camera.

A second four-strip framing camera imaged the resolution target placed between the pinhole and the detector. This camera was positioned on-axis with the backlighter target normal, at a distance of 229 mm from target chamber center. A protective snout with an open aperture (ie, no additional pinhole mask) was placed in front of the framing camera. A blast shield was placed at the front of the snout of 254 μm-thick beryllium to help protect the camera from target debris. Additionally, another 508 μm Be and 25.4 μm zinc were used as a rear filter for the camera. This filtering prevents most of the signal from below 5 keV from reaching the detector. The image of the resolution target was large enough that it spanned all four strips, with each strip imaging a different section of the grid at different times.

III. RESULTS

Figure 3a shows images of the laser spot at 7.5 ns. Figure 3b shows an image of the resolution grid at the same time on the same shot. Spatial scales are shown for each image.

At t= 1.5 ns, the bright zinc emission spot in Figure 3a is 220 μm FWHM, and well centered between the two gold blow-off signals and therefore well-centered over the pinhole aperture. After flat-fielding, the images in strips 1 and 3 (at t = 1.5 ns) are the same intensity to within 8%. At later times, the center of the spot moves less than 30 μm from it's position over the pinhole aperture, but does get larger and dimmer by 30%. At t= 7.5 ns, the full-width, half-max spot size has expanded to 320 μm. The bright gold fiducial signal is present only for t = 1-2 ns, and so are not visible in Figure 3a.

At t = 1.5 ns in the flat-fielded image of the resolution grid strip 3 is slightly brighter ($\sim$ 5% of the total de-

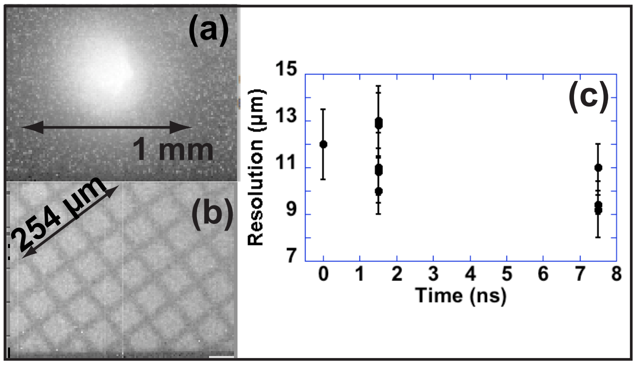

FIG. 3: Framing camera images at 7.5 ns of the laser-driven spot (a) and the resolution grid (b). Images confirm that the emitting spot stays centered over the pinhole aperture, and that x-rays make it through the pinhole to image the target. (c) Resolution of grid wires as a function of time. Late time shows slight improvement in the resolution, indicating minimal pinhole closure.

tected signal) than strip 1, indicating some spatial variation in the spot brightness. From simulations, we expect a source intensity variation over the image of less than 25%. At $t = 7.5$ ns, the signal level in the image of the grid is lower, but only by as much as the emitting spot is dimmer, 25% of the total signal level.

At $t = 1.5$ ns the grid wires are imaged with a resolution of 11.5 ± 0.7 μm. At $t = 7.5$ ns, the wires are imaged with a resolution of 9.9 ± 0.7 μm. Resolution of the grid wires plotted as a function of time are shown in Figure 3c. The resolution of the wire target was significantly smaller than the pinhole diameter at early times because the high aspect ratio of the pinhole (20 μm diameter, 75 μm long) caused vignetting, resulting in a smaller effective source size. A changing wire resolution, along with dimming of the detected signal and no dimming of the source image would have been taken as indicators that the radiation from the emitter material was causing pinhole closure. Here, the resolution of the target did not change markedly, and so we conclude that there was little-to-no pinhole closure.

IV. CONCLUSION

We have fielded a pinhole-apertured point-projection backlighter on Omega to image a gold resolution grid at high magnification. Using framing cameras, we have imaged the resolution target at 7.5 ns, showing that the x-ray signal remains on and centered over the target aperture, and that the aperture does not close significantly. The measured resolution of the grid wires did not change by an amount greater than the error bars between 1.5 ns and 7.5 ns. This resolution was limited by the size of the pinhole acting as an aperture of the source.

This backlighter will be fielded on NIF imaging a resolution target at high magnification before being used in an actual experiment. This step is necessary to examine debris patterns with the higher drive energy available on NIF, as well as testing target, diagnostic, and beam pointing capabilities.

The authors would like to acknowledge the Omega technical staff, without whom the execution of these experiments would be impossible. Thanks also to Jim Knauer for advice concerning the safe operation of the framing cameras with pinhole-apertured backlighters. This work was performed under the auspices of the U.S. Department of Energy by Lawrence Livermore National Laboratory under Contract DE-AC52-07NA27344.

[1] D. K. Bradley, O. L. Landen, A. B. Bullock, S. G. Glendinning, and R. E. Turner, Optics Let. **27**, 134 (2002).

[2] J. Workman, J. R. Fincke, G. A. Kyrala, and T. Pierce, Appl. Opt. **44**, 859 (2005).

[3] B. E. Blue, H. F. Robey, S. G. Glendinning, M. J. Bono, S. C. Burkhart, J. R. Celeste, R. F. Coker, R. L. Costa, S. N. Dixit, J. M. Foster, et al., Phys. Plasmas **12**, 6313 (2005).

[4] B. E. Blue, S. V. Weber, S. G. Glendinning, N. E. Lanier, D. T. Woods, M. J. Bono, S. N. Dixit, C. A. Haynam, J. P. Holder, D. H. Kalantar, et al., Phys. Rev. Let. **94**, 095005 (2005).

[5] C. C. Kuranz, B. E. Blue, R. P. Drake, H. F. Robey, J. F. Hansen, J. P. Knauer, M. J. Grosskopf, C. Krauland, and D. C. Marion, Rev. Sci. Inst. **77**, 327 (2006).

[6] O. L. Landen, D. R. Farley, S. G. Glendinning, L. M. Logory, P. M. Bell, J. A. Koch, F. D. Lee, D. K. Bradley, D. H. Kalantar, C. A. Back, et al., Rev. Sci. Inst. **72**, 627 (2001).

[7] A. B. Bullock, O. L. Landen, and D. K. Bradley, Rev. Sci. Inst. **72**, 690 (2001).

[8] A. B. Bullock, O. L. Landen, B. E. Blue, J. Edwards, and D. K. Bradley, J. Appl. Phys. **100**, 3301 (2006).

[9] B. E. Blue, J. F. Hansen, M. T. Tobin, D. C. Eder, and H. F. Robey, Rev. Sci. Inst. **75**, 4775 (2004).

[10] T. R. Boehly, R. S. Craxton, T. H. Hinterman, J. H. Kelly, T. J. Kessler, S. A. Kumpan, S. A. Letzring, R. L. McCrory, S. F. B. Morse, W. Seka, et al., Rev. Sci. Inst. **66**, 508 (1995).

[11] D. K. Bradley, P. M. Bell, J. D. Kilkenny, R. Hanks, O. Landen, P. A. Jaanimagi, P. W. McKenty, and C. P. Verdon, Rev. Sci. Inst. **63**, 4813 (1992).

[12] O. L. Landen, P. M. Bell, J. A. Oertel, J. J. Satariano, and D. K. Bradley, in *Proc. SPIE Vol. 2002, p. 2-13, Ultrahigh- and High-Speed Photography, Videography, and Photonics '93, Paul W. Roehrenbeck; Ed.*, edited by P. W. Roehrenbeck (1993), vol. 2002 of *Presented at the Society of Photo-Optical Instrumentation Engineers (SPIE) Conference*, pp. 2–13.